JOURNAL OF APPLIED PHYSICS VOLUME 88, NUMBER 7 1 OCTOBER 2000

# Variable-range hopping conductivity and magnetoresistance in $n$-$CuGaSe_2$

K. G. Lisunov and E. Arushanov
*Institute of Applied Physics, Academy of Sciences of the Moldova Republic, Academiei Str. 5, Kishinev 277028, Moldova*

G. A. Thomas
*George R. Harrison Spectroscopy Laboratory, Massachusetts Institute of Technology, Cambridge, Massachusetts 02139*

E. Bucher
*Universität Konstanz, Fakultät für Physik, Postfach X 916, D-78457 Konstanz, Germany*

J. H. Schön[a)]
*Bell Laboratories, Lucent Technologies, 600 Mountain Avenue, Murray Hill, New Jersey 07974-0636*

(Received 17 April 2000; accepted for publication 5 July 2000)

The low-temperature charge transport in $n$-$CuGaSe_2$ was investigated in zero and nonzero magnetic field. Both the Mott as well as the Shklovskii–Efros regimes of the variable-range hopping are observed in different temperature intervals. The complete set of the parameters describing the properties of the localized electrons (the localization radius, the dielectric permeability, the width of the Coulomb gap, and the values of density of states at the Fermi level) are obtained by analysis of the conductivity in zero field, on one hand, and the positive magnetoresistance in a small field, on the other hand. The negative magnetoresistance in low fields is observed in all specimens in both hopping regimes. Moreover, it is interpreted as a result of quantum interference between different paths of the tunneling electrons in conditions of scattering by intermediate centers. © *2000 American Institute of Physics.* [S0021-8979(00)00720-9]

## I. INTRODUCTION

$CuGaSe_2$ (CGS), belonging to the I–III–$VI_2$ family of chalcopyrite compounds, has been studied as a very promising material for photovoltaic applications. Efficiencies exceeding 9% have been obtained for single crystal as well as thin film solar cells.[1,2]

Recently, it has been demonstrated that $n$-type CGS can be achieved by codoping with Ge and Zn.[3] The samples have been doped with Ge by ion implantation and posttreated in a Zn atmosphere. Room temperature carrier concentrations up to $10^{17}\,cm^{-3}$ have been reported. The preparation of $n$-type $CuGaSe_2$ might be helpful by improving the efficiency of photovoltaic devices using homojunctions and therefore reducing the interface recombination of conventional heterojunction solar cells ($CuGaSe_2$/CdS/ZnO).

The Hall effect, the electrical conductivity, and the charge carrier mobility of $n$-type $CuGaSe_2$ single crystals were studied in the temperature range between 2 and 300 K.[4] The values of the gap between the conduction band and the impurity band, the concentration of donors, and of compensating acceptors were determined. Moreover, the mobility above 100 K was described by scattering of conduction band electrons at phonons and impurities.

In this article, we report for the measurements of the low-temperature (down to $T=2\,K$) conductivity of $n$-$CuGaSe_2$ single crystals in zero and nonzero magnetic fields. The purpose of the work is to investigate variable-range hopping conductivity of this compound. Analysis of the experimental data is performed to determine parameters of the localized electrons such as the localization radius, the dielectric permeability, the density of states at the Fermi level and the width of the Coulomb quasigap. Additionally, a negative magnetoresistance is observed and analyzed using different models of quantum interference between the hopping electrons.

## II. CRYSTAL GROWTH AND EXPERIMENTAL METHODS

$CuGaSe_2$ single crystals were grown by chemical vapor transport using iodine as a transport agent. Ge ion implantation (dose of $1-5\times10^{15}\,cm^{-2}$, acceleration voltage 200 kV) was performed on Cu-annealed (500 °C/120 h) single crystals. In order to achieve $n$-type conduction the samples were annealed in the presence of Zn.[3] Samples No. $L_1$ and No. $L_2$ were annealed for 10 min (rapid thermal annealing) to heal the implantation damage, whereas samples No. 3 and No. 4 were slowly ramped to the annealing temperature and held at the elevated temperature for 1 h. The parameters are summarized in Table I. The magnetotransport properties of the $CuGaSe_2$ samples were measured in the temperature range from 2 to 100 K at magnetic fields up to 8 T using a conventional dc setup for Hall and resistivity measurements. Parameters such as donor concentration $N_d$ and degree of compensation $K$ were calculated using the procedure presented in Refs. 4 and 5.

## III. EXPERIMENTAL RESULTS

The temperature $T$ dependence of the conductivity $\sigma$ of the investigated $n$-$CuGaSe_2$ crystals is shown in Fig. 1(a), and $\sigma$ vs $1/T$ is displayed in Fig. 1(b). It is evident that the

[a)]Electronic mail: hendrik@lucent.com

 © 2000 American Institute of Physics

Downloaded 13 Apr 2004 to 130.232.104.240. Redistribution subject to AIP license or copyright, see http://jap.aip.org/jap/copyright.jsp

TABLE I. Doping parameters (implantation dose, acceleration voltage, annealing time and temperature) for the investigated $n$-$CuGaSe_2$ single crystals.

| Sample No. | Dose ($cm^{-2}$) | Acc. voltage (kV) | Time (min) | Temperature (°C) |
|---|---|---|---|---|
| $L_1$ | $10^{15}$ | 150 | 10 | 380 |
| $L_2$ | $10^{15}$ | 150 | 10 | 400 |
| 3 | $10^{15}$ | 200 | 60 | 400 |
| 4 | $5\times10^{15}$ | 200 | 60 | 400 |

conductivity of $CuGaSe_2$ has an activated character, including two intervals with different slopes of the function of $\sigma(1/T)$ [Fig. 1(b)]. The first one, at high temperatures, is connected with the band conduction (activation of electrons from donor levels to the conduction band) while the second one, on the low-temperature side, is determined by the hopping conductivity, or transitions between the impurity centers or localized states inside the impurity band. The low-temperature slope is not constant but varies with $T$ suggesting variable-range hopping (VRH) conduction. The resistivity versus magnetic field $B$ is shown in Fig. 2 (No. $L_1$) and in Fig. 3 (No. 3) for different temperatures. The dependence of $\ln \rho(B)/\rho(0)$ on $B$ for No. 4 is quite similar to that of No. 3 (Fig. 3). At small magnetic fields $B$ the magnetoresistance (MR) is negative MR (NMR) for all investigated specimens reaching a maximum value of ~20% for No. $L_1$ (Fig. 2) and ~5%–10% for No. 3 (Fig. 3) and No. 4. When $B$ is increased positive MR (PMR) is observed up to the highest applied field (8 T). In addition, both contributions to the MR, the NMR, and the PMR, depend significantly on temperature.

## IV. DISCUSSION

### A. VRH conductivity of *n*-CGS for *B*=0

If it is energetically favorable for localized electrons to hop beyond the nearest-neighbor impurity centers, so that the average hopping length exceeds the average distance between the donors, VRH conductivity sets in.[6] In conditions of *strong localization*, $N_d^{1/3}\xi \sim N_d^{1/3} a_B \ll 1$ (where $N_d$ is the concentration of the donor impurities, $\xi$ is the localization radius, i.e., the length where the wave function of the localized electron is not exponentially small, and $a_B$ is the Bohr radius) VRH can only be observed within a relatively small temperature interval of hopping conduction. Otherwise, or more strictly, if $N_d^{1/3}\xi \leqslant 0.25$ [the regime of the *Anderson localization*, which takes place near the metal–insulator transition (MIT)] VRH conduction can be observed inside the whole interval of the hopping conductivity.[6]

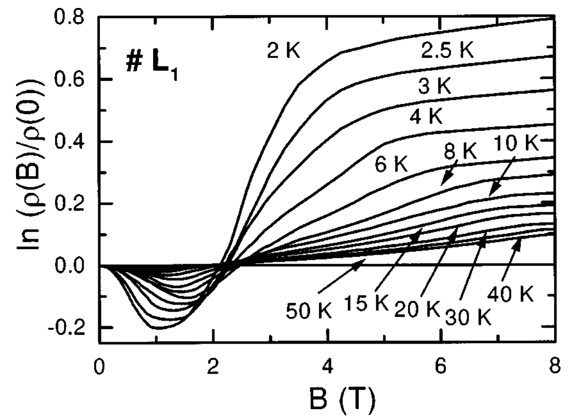


FIG. 2. MR $\rho(B)$ of sample No. $L_1$ as function of magnetic field $B$ for various temperatures from 2 to 50 K.

Two different types of VRH should be distinguished. Mott ($M$)-type VRH takes place when the electron density of states (DOS) $g(\mu)$, at the Fermi level $\mu$ is constant,[6,7] and Shklovskii–Efros (SE)-type of VRH is found when the DOS has a parabolic quasigap due to the long-range Coulomb correlations of the localized electrons in the energy range between $\mu-\Delta$ and $\mu+\Delta$.[8] The conductivity $\sigma$ can be expressed in both cases of VRH as

$$\sigma(T)=\sigma_0 \exp\left[\left(\frac{T_{0p}}{T}\right)^{1/p}\right], \tag{1}$$

where the prefactor $\sigma_0$ depends only weakly on $T$, $T_{0p}$ is the characteristic hopping temperature, with $p=2$ in the SE–VRH or $p=4$ in the M–VRH regimes, respectively. The characteristic temperature, $T_{0p}$, for both cases of VRH conduction can be expressed as[7,8]

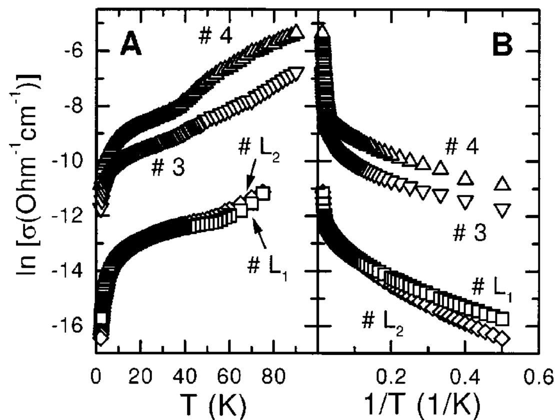


FIG. 1. Temperature dependence of the conductivity $\sigma$ of the investigated $n$-$CuGaSe_2$ single crystals. (a) $\sigma$ vs $T$ and (b) $\sigma$ vs $1/T$.

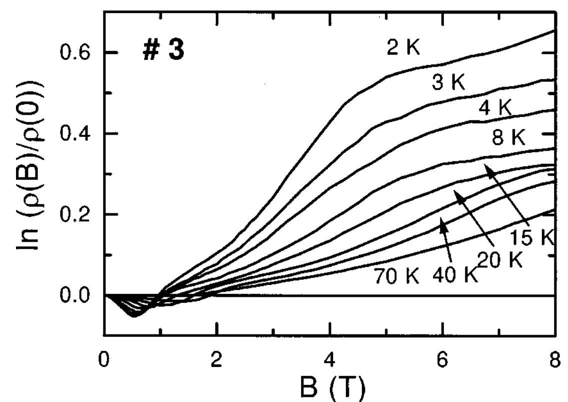


FIG. 3. MR $\rho(B)$ of sample No. 3 as function of magnetic field $B$ for various temperatures from 2 to 70 K.

Downloaded 13 Apr 2004 to 130.232.104.240. Redistribution subject to AIP license or copyright, see http://jap.aip.org/jap/copyright.jsp

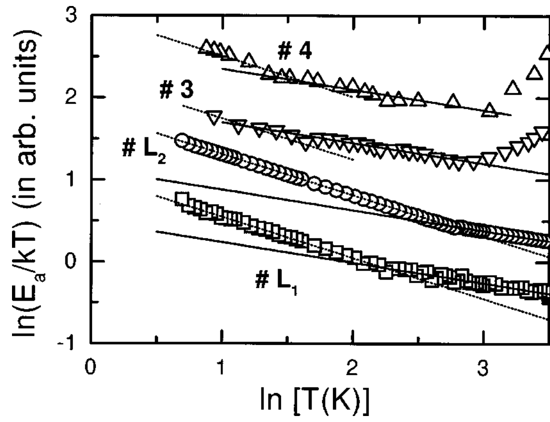


FIG. 4. Local activation energy $E_a$ [$E_a = -d\ln(\sigma)/d(k_BT)^{-1}$] vs ln $T$. The dashed lines correspond to a slope of −1/2 and −1/4, respectively. They correspond to the regimes of SE- and M-type VRH.

$$T_{04}=\frac{\beta_4}{k_B g(\mu)\xi^3},\quad T_{02}=\frac{\beta_2}{k_B\kappa\xi},\tag{2}$$

where $\beta_4 = 21\pm1$, $\beta_2 = 2.8$, and $\kappa$ is the dielectric permeability.

Assuming a rectangular shape of DOS in the interval $\mu-\Delta E$, $\mu+\Delta E$ for simplicity reasons, $g(\mu)$ can be written as

$$g(\mu)=\begin{cases}N_d/(2\Delta E), & |E-\mu|\le\Delta E\\ 0, & |E-\mu|>\Delta E\end{cases},\tag{3}$$

and the temperature of the onset of M–VRH $T_{v4}$ can be obtained by[8]

$$T_{v4}=\frac{\Delta E N_d^{1/3}\xi}{(2\beta_4)^{1/3}k_B}.\tag{4}$$

The temperature of the transition to VRH conduction over states of the Coulomb gap (SE regime), or the opening of the Coulomb gap, can be expressed as follows:[8]

$$T_{v2}=\frac{N_d^{2/3}\xi e^2}{2\kappa k_B}.\tag{5}$$

The values of the width of the quasigap, $\Delta$, and the DOS outside the gap, $g_0$, are given by[8,9]

$$\Delta=\frac{k_B}{2}\sqrt{T_{02}T_{v2}},\quad g_0=\frac{k_B^2\kappa^3T_{02}T_{v2}}{16e^2}.\tag{6}$$

The type of hopping conduction can be determined from the experimental data by analyzing the local activation energy, $E_a$[8] (which is defined as $E_a = -d\ln(\sigma)/d(k_BT)^{-1}$) using the universal relation $\ln(\sigma)\sim T^{1/p}$. The value of $p$ can be obtained from the slope of the plot $\ln(E_a/k_BT)$ vs ln $T$ (see Fig. 4).

A simple estimation for the DOS at the Fermi level $\mu$ can be obtained using the following approximation:[8]

$$g(\mu)\approx\frac{KN_d}{E_0},\tag{7}$$

where $E_0 = e^2/(\kappa_0 r_d)$ is the energy of the Coulomb repulsion, $r_d = (4\pi N_d/3)^{-1/3}$ is the half of the mean distance between the donors, $K$ is the degree of the compensation, and $\kappa_0\approx13.6$ is the dielectric permeability of $CuGaSe_2$, far from MIT.

As evident from Fig. 4, both VRH regimes can be found in all investigated specimens. However, in No. $L_1$ and No. $L_2$ the SE regime is observed much more clearly than in samples No. 3 and No. 4, respectively. In the latter case SE–VRH covers only the smaller part of the interval of the hopping conduction at the lowest investigated temperatures (below 5 K). The parameters $T_{02}$, $T_{04}$, $T_{v2}$, and $T_{v4}$ can be obtained with sufficient accuracy by plotting of ln $\sigma$ vs $T^{1/p}$ (not shown) using Eq. (1). Their values are summarized in Table II.

Using Eqs. (2), (4), and (5) one can easily derive the corresponding expressions for the localization radii $\xi_M$, $\xi_{SE}$ (where the subscript M and SE refer to the VRH regimes in which the value of the localization radius are obtained), the DOS at the Fermi level $g(\mu)$, and the dielectric permeability $\kappa$ as follows:[10]

$$g(\mu)=\frac{N_d}{2k_B(T_{v4}^3T_{04})^{1/4}},\tag{8}$$

$$\xi_M=\frac{\beta_4^{1/3}}{[k_BT_{04}g(\mu)]^{1/3}},\tag{9}$$

$$\kappa=\frac{e^2N_d^{1/3}\beta_2^{1/2}}{k_B(2T_{02}T_{v2})^{1/2}},\tag{10}$$

$$\xi_{SE}=\frac{\beta_2e^2}{T_{02}\kappa k_B}.\tag{11}$$

The values of $\Delta$ and $g_0$ can be calculated using Eq. (6). All these parameters are summarized in Table II.

First of all, it should be pointed out that both $\xi_M$ and $\xi_{SE}$ for samples No. $L_1$ and No. $L_2$ are much higher than those found for No. 3 and No. 4. On the other hand, the values of $T_{02}$ and, especially, $T_{04}$, are quite comparable for all

TABLE II. Parameters describing the properties of localized electrons in $n$-$CuGaSe_2$ determined from the transport data in zero field [donor concentration $N_d$, degree of compensation $K$, characteristic hopping temperatures $T_{vp}$, density of states at the Fermi level $g(\mu)$, density of states outside the Coulomb gap $g_0$, density of states calculated using Eq. (7) $g^{calc}$, localization radii $\xi$, dielectric permeability $\kappa$, and Coulomb gap $\Delta$].

| Sample No. | $N_d$ ($10^{16}$ cm$^{-3}$) | $K$ (%) | $T_{v2}$ (K) | $T_{v4}$ (K) | $T_{02}$ (K) | $T_{04}$ (K) | $g(\mu)$ ($10^{16}$ cm$^{-3}$ meV$^{-1}$) | $g_0$ ($10^{16}$ cm$^{-3}$ meV$^{-1}$) | $g^{calc}$ ($10^{16}$ cm$^{-3}$ meV$^{-1}$) | $\xi_M$ (Å) | $\xi_{SE}$ (Å) | $\kappa$ | $\Delta$ (meV) |
|---|---|---|---|---|---|---|---|---|---|---|---|---|---|
| $L_1$ | 0.54 | 33 | 9 | 50 | 33 | 1840 | 0.026 | 0.036 | 0.061 | 810 | 730 | 20 | 0.76 |
| $L_2$ | 0.98 | 22 | 15 | 47 | 55 | 3140 | 0.042 | 0.039 | 0.060 | 580 | 590 | 14 | 1.25 |
| 3 | 12 | 83 | 4 | 22 | 15 | 1040 | 1.2 | 1.8 | 1.2 | 270 | 250 | 124 | 0.33 |
| 4 | 19 | 85 | 5 | 25 | 19 | 940 | 1.8 | 2.3 | 1.9 | 250 | 220 | 116 | 0.42 |

Downloaded 13 Apr 2004 to 130.232.104.240. Redistribution subject to AIP license or copyright, see http://jap.aip.org/jap/copyright.jsp

samples, despite of the profound differences between $N_d$ for the pairs of samples No. $L_1$ and No. $L_2$ and samples No. 3 and No. 4, respectively. Furthermore, comparable values of $\xi$ have been obtained for No. 3 and No. 4, in good agreement with the observation of similar values of $T_{02}$ and $T_{04}$ and those of $N_d$. This allows us to suppose that the earlier method to determine of the characteristic parameters given in Eqs. (8)–(11) can be applied only to No. 3 and No. 4, but not to No. $L_1$ and No. $L_2$. A possible reason may be the different methods of preparation, especially the differences in the postimplantation annealing of these specimens, that may lead, e.g., to the formation of impurity clusters or some additional defects in samples No. $L_1$ and No. $L_2$. In such a case it may not be applicable to assume a homogeneous distribution of impurities in order to obtain values for $N_d$ and $K$. This could lead to the observed disagreements. On the other hand, we can compare the results listed above for No. 3 and No. 4 (Table II) with those found for No. 7 of $CuGaSe_2$ in Ref. 11 (in the M–VRH regime) with a comparable value of $N_d = 9.6\times 10^{16}\,\mathrm{cm}^{-3}$ and similarly $K = 54\%$: $T_{04} = 580\,\mathrm{K}$, $T_{v4} = 19\,\mathrm{K}$, and $\xi_M = 290\,\mathrm{Å}$. The agreement between these data and those obtained for No. 3 and No. 4 (Table II) is quite satisfactory to conclude that Eqs. (8)–(11) give reasonable estimations for the corresponding parameters. Moreover, the estimations of the DOS by Eq. (7) correlates well with both values of $g(\mu)$ and $g_0$ found for these samples.

In the following subsection we will apply an additional method to determine the localization radius $\xi$, the DOS, and the permeability $\kappa$. However, this technique does not involve the utilization of the values of $N_d$ and $K$. We will show that more consistent values of $\xi$ are obtained for all investigated specimens. Although the agreement between $\xi_M$ and $\xi_{SE}$ will not be as good as that displayed in Table II, a reasonable explanation of this particular disagreement will be proposed.

## B. PMR of *n*-$CuGaSe_2$

As mentioned earlier (Sec. II), a transition from the relatively small initial NMR to a much larger PMR is observed (Figs. 2 and 3), when $B$ is increased. PMR in the hopping regime is determined by a shrinkage of the electronic wave functions perpendicular to the field[8] and exhibits, generally, an exponential type of dependence on $B$.[8] However, this dependence is different for the different field strengths. Additionally, PMR in the VRH regime in an arbitrary field can depend strongly on the scattering of hopping electrons by intermediate impurity centers, resulting in a more complex dependence on $B$.[12] On the other hand, PMR has a universal (and rather simple) field and temperature dependence in weak fields, given by the condition $\lambda \gg \xi$ [where $\lambda = (\hbar/eB)^{1/2}$ is the magnetic length],[8,12] which does not contain any scattering parameters. Moreover, important information about the localization radius and DOS can be obtained by analyzing PMR in weak fields. Therefore, later we will restrict our analysis of PMR to the interval of a weak magnetic field. Furthermore, we will compare the values estimated by this method with those obtained in the previous subsection.

In a weak field PMR satisfies the following equation:[8]

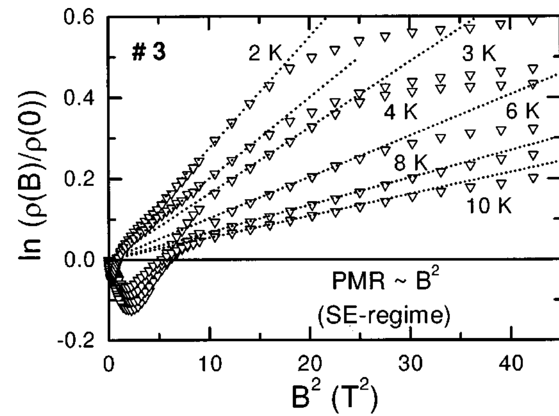


FIG. 5. PMR in the SE regime for sample No. 3. The quadratic field dependence is clearly observable.

$$\ln\frac{\rho(B)}{\rho(0)} = A_p(T)B^2, \qquad (12)$$

where $A_p$ is given by

$$A_p(T) = A_{p0}T^{-3/p} \qquad (13)$$

and $A_{p0}$ can be expressed as

$$A_{p0} = t_p\frac{\xi^4 e^2 T_{0p}^{3/p}}{\hbar^2}, \qquad (14)$$

where $t_2 = 0.0015$ and $t_4 = 5/2016$ are the constants.

Hence, a plot of $\ln \rho(B)/\rho(0)$ vs $B^2$ in low fields should result in a straight line starting from the origin according to Eq. (12). Here we suppose, first, that the NMR and PMR contributions to MR are additive, and, next, that NMR saturates with increasing $B$. Therefore, the contribution of NMR can be neglected when the field is increased. As evident from Figs. 5 and 6, all these conditions are satisfied quite well for all investigated specimens. In both VRH regimes we observe a quadratic field dependence of the PMR in agreement with Eq. (12). The dependencies of $A_p(T)$ vs $T^{3/p}$ are linear functions (see Fig. 7). However, the plots of $A_2(T)$ vs $T^{3/2}$ for No. 3 and No. 4 do not start from the origin suggesting, at a first glance, an additional temperature-independent contribution to the PMR. On the other hand, one should take into

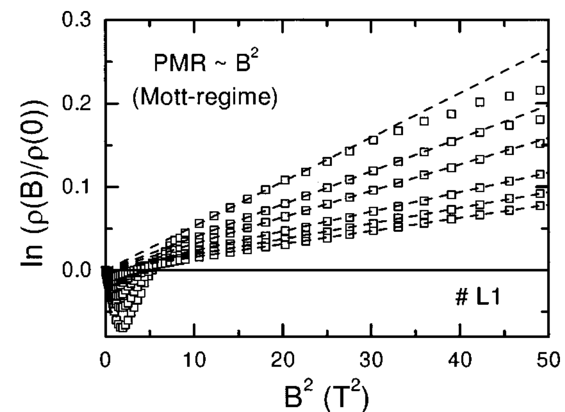


FIG. 6. PMR in the M regime for sample No. $L_1$. The quadratic field dependence is clearly observable.

Downloaded 13 Apr 2004 to 130.232.104.240. Redistribution subject to AIP license or copyright, see http://jap.aip.org/jap/copyright.jsp

account the wider region of the M–VRH for these specimens as compared with relatively small interval of SE–VRH, whereas for No. $L_1$ the intervals of both VRH regimes are similar (Fig. 4). This may shift the starting point of the dependence given by Eq. (13) for $p=2$ for No. 3 and No. 4 while for No. $L_1$ such shift is negligible. The values of $A_{p0}$ are summarized in Table III. Also, in Table III, values of $\xi_M$ and $\xi_{SE}$ using Eq. (14), $g(\mu)$ and $\kappa$ evaluated by Eq. (2), and $g_0$ calculated with the second of Eq. (6) are displayed. A comparison of the data of Tables II and III reveals that the values of $\xi_{SE}$ for No. 3 and No. 4 obtained by both methods agree well. Furthermore, no inconsistency between the values of this parameter for No. 3 and No. 4, on one hand, and for No. $L_1$, on the other hand, is observed in Table III. (They are quite comparable, as expected from the similarity of $T_{op}$ for all specimens.) However, the values of $\xi_M$ in Table III are systematically and measurably lower than those of $\xi_{SE}$. The reason for this disagreement is obvious and implies that DOS does not have a perfect rectangular shape (as has been assumed for M–VRH conduction) but contains a gap near the Fermi level (which leads to the SE–VRH). Therefore, analysis in the M–VRH regime implies a systematic inaccuracy, which will be larger the broader the Coulomb gap, and consequently, the larger interval of SE–VRH compared to the M–VRH regime is. The difference between $\xi_M$ and $\xi_{SE}$ is largest for No. $L_1$ in accordance with the largest value of $\Delta$ (among samples No. $L_1$, No. 3, and No. 4, see Table II). One can also observe the measurable discrepancy between $g(\mu)$ and $g_0$ in Table III, which is related to the same reason. However, the values of $g(\mu)$ and $g_0$ must be comparable. Taking this into account and the fact that $T_{04}\sim 1/[g(\mu)\xi^3]$, we can expect that both ratios, $[g(\mu)/g_0]^{1/3}$ and $\xi_{SE}/\xi_M$, would be similar, too. As evident from Table II, this relation is satisfied within an error of ~8%–15%. Finally, we would like to mention good agreement between the values of $\kappa$ for No. 3 and No. 4 obtained with both methods.

To conclude, although the interval of SE–VRH in samples No. 3 and No. 4 is relatively narrow, the most accurate data on $\xi$ and $\kappa$ in $CuGaSe_2$ can be estimated in this interval by both methods. The first method is more appropriate for determination of DOS in both VRH regimes. Taking this into account, we obtain the complete and consistent set of parameters characterizing the properties of the localized electrons in $n$-$CuGaSe_2$. However, for samples No. $L_1$ and No. $L_2$ the first method is found not to be inapplicable, suggesting significant differences between them and No. 3 and No. 4 probably due to different crystal growth methods.

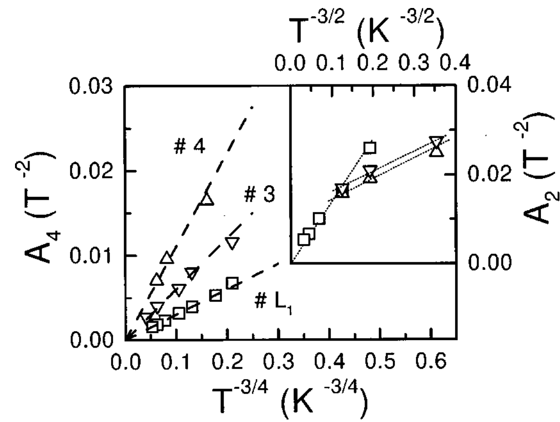


FIG. 7. Parameters $A_4$ and $A_2$ describing the temperature dependence of the positive MR in the M and SE regime, respectively, as function of temperature.

### C. NMR of $n$-$CuGaSe_2$

In this subsection we analyze NMR observed at small fields in samples No. $L_1$, No. 3, and No. 4 (Figs. 2 and 3). It can be expected that in nonmagnetic semiconductors NMR has the orbital nature. Moreover, it is generally believed that in the VRH region this phenomenon is connected with quantum interference (QI) between hopping electrons.[12] Extensive experimental investigations in different semiconductors have proved this point of view. However, different theoretical approaches to QI in the VRH region were put forward in order to interpret NMR. Excluding perhaps a narrow interval in the vicinity of the MIT,[13] it is now widely accepted that NMR in the VRH regime is a consequence of QI between different paths, which are formed due to scattering of the tunneling electron by intermediate scattering centers. These centers are located within a cigar-shaped volume of the characteristic length $R$ and the transversal radius $(R\xi)^{1/2}$, where $R$ is the hopping length.[12] Two theoretical approaches to QI can be formulated, depending on how many scattering centers (or scattering acts) are included inside the volume $\sim R(R\xi)^{1/2}$, or in other words, on the degree and nature of disorder in the material

(i) In doped crystalline semiconductors the disorder originates presumably from the randomness of the positions of doping atoms. In this case, the same type of atom serves both for hopping and for scattering. Therefore, it can be shown that the number of scattering centers would be of

TABLE III. Parameters describing the properties of localized electrons in $n$-$CuGaSe_2$ determined from the positive magnetoresistance [characteristic of the temperature dependence of PMR $A_{vp}$, localization radii $\xi$, density of states at the Fermi level $g(\mu)$, density of states outside the Coulomb gap $g_0$, and dielectric permeability $\kappa$].

| Sample No. | $A_{20}$ ($T^{-2}K^{3/2}$) | $A_{40}$ ($T^{-2}K^{3/4}$) | $\xi_M$ (Å) | $\xi_{SE}$ (Å) | $g(\mu)$ ($10^{16}$ cm$^{-3}$ meV$^{-1}$) | $g_0$ ($10^{16}$ cm$^{-3}$ meV$^{-1}$) | $\kappa$ | $[g(\mu)/g_0]^{1/3}$ | $\xi_{SE}/\xi_M$ |
|---|---|---|---|---|---|---|---|---|---|
| $L_1$ | 0.14 | 0.030 | 120 | 220 | 8.3 | 1.4 | 66 | 1.8 | 1.8 |
| 3 | 0.045 | 0.049 | 150 | 220 | 7.4 | 3.7 | 145 | 1.3 | 1.5 |
| 4 | 0.047 | 0.046 | 150 | 200 | 8.1 | 4.5 | 124 | 1.2 | 1.3 |

Downloaded 13 Apr 2004 to 130.232.104.240. Redistribution subject to AIP license or copyright, see http://jap.aip.org/jap/copyright.jsp

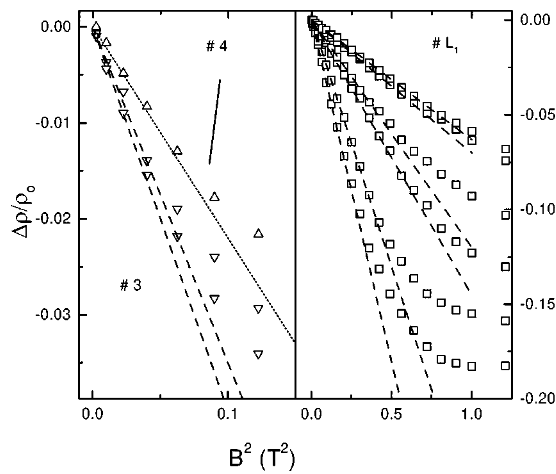


FIG. 8. NMR of samples No. 3, No. 4 (left), and No. L1 at small fields at low temperatures (SE regime). The dashed lines correspond to a quadratic fit.

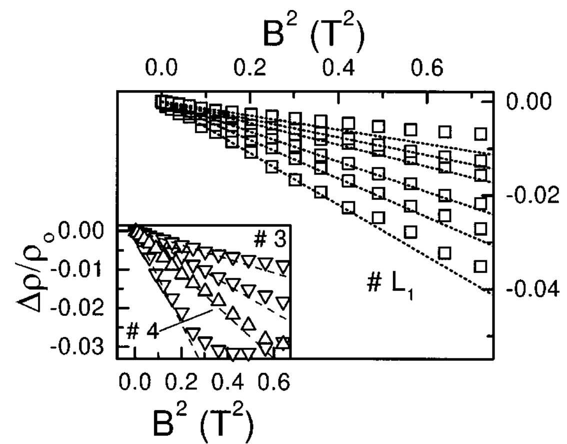


FIG. 9. NMR of samples No. 3, No. 4 (left), and No. $L_1$ at small fields in the M regime. The dashed lines correspond to a quadratic fit.

order unity. This situation was analyzed first in Ref. 14 and the theory was further developed in Ref. 15.

(ii) A second class of materials (including, e.g., amorphous or polycrystalline semiconductors) contains a large number of defects which do not produce localized states in the vicinity of the Fermi level but can scatter a tunneling electron. As a result multiple scattering can be expected, using the approach that was developed in Refs. 16 and 17.

In order to distinguish between these two situations, it is convenient to analyze NMR in the limit of very small fields which is defined by the condition that the magnetic flux through the interference area $R^{1/2}\xi$ is comparable with the flux quantum $\phi_0$.[12,18] In this case $\Delta\rho(B)/\rho(0)$ has a simple form, similar for both approaches

$$\frac{\Delta\rho(B)}{\rho(0)}=f(T)B^2, \tag{15}$$

where $f(T)\sim T^{-q}$.

In the second case (ii) the exponent $q=3/p$ depends on the regime of VRH, whereas in the first case (i) $q=1$ is the same in both VRH regimes. Additionally, for this case simple equations for the characteristic fields in the M–VRH regime, $B_{\max}(T)\approx 0.8\,B_0(T)$ and $B_{\text{zero}}(T)\approx 1.3\,B_0(T)$, where $B_{\max}$ and $B_{\text{zero}}$ are the fields at which $\Delta\rho(B)/\rho(0)$ attains the maximum absolute value or changes the sign, respectively, are predicted [with $B_0=4\hbar T^{3/8}/(\xi^2 eT_{04})^{3/8}$]. Experimentally, slightly different values of the exponent $q$ are reported for various materials, including $q=0.77$ and 0.83 similar to that of the case (ii) in the M–VRH in $n$-$CuInSe_2$,[19] and $q=1.2$ in $n$-GaAs,[20] and 1.3 in $n$-CdSe[21] similar to $q=1$ in the case (i).

As shown in Figs. 8 and 9, the quadratic field dependence of NMR is well observed in both VRH regimes for all investigated specimens. The criterion of the very weak field is well satisfied also. The functions $f(T)$, obtained from Figs. 8 and 9 for each specimen are displayed in Fig. 10. As seen from this figure, the values of the exponent $q=1$ are the same for No. 3 and No. 4 in both VRH regimes. In addition, excellent agreement with the predictions earlier for $B_{\max}(T)$ and $B_{\text{zero}}(T)$ is observed for both specimens No. 3 and No. 4 in the M–VRH interval (see Fig. 11). Hence, we can conclude that NMR in these samples takes place in conditions of the regime of single scattering (case i). On the other hand, for No. $L_1$ the situation is quite different. As predicted for the case (ii), $q=3/2$ and 3/4 are observed in the SE– and M–VRH regions, respectively, while the temperature dependence of both characteristic fields, $B_0$ and $B_{\max}$, is in contrast to the prediction in case (i) except for a small interval between $T\approx 40$–50 K. This allows us to establish that the properties of sample No. $L_1$ are governed by multiple scattering (case ii). A possible reason for such nonuniversal behavior in one and the same material may be different conditions in which the samples No. $L_1$, No. 3 and No. 4 have been obtained. Disorder and defects might arise from residual implantation damage due to the short annealing procedure.

## V. CONCLUSIONS

VRH conduction in $n$-$CuGaSe_2$ in zero and nonzero magnetic field was investigated. Both VRH regimes, M and SE, are observed in different temperature intervals. The complete set of the parameters describing the properties of local-

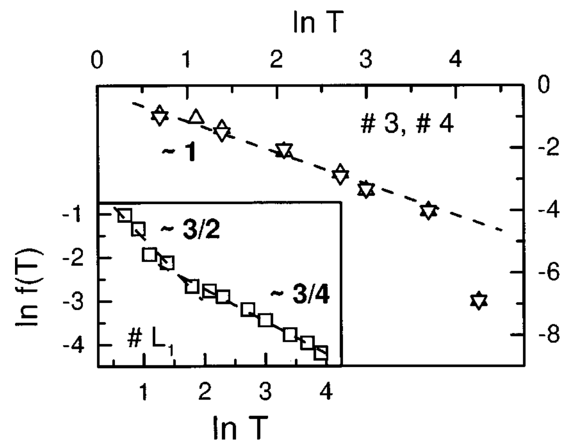


FIG. 10. Temperature dependence of the prefactor of the quadratic NMR for samples No. $L_1$ (inset) and No. 3 and No. 4.

Downloaded 13 Apr 2004 to 130.232.104.240. Redistribution subject to AIP license or copyright, see http://jap.aip.org/jap/copyright.jsp

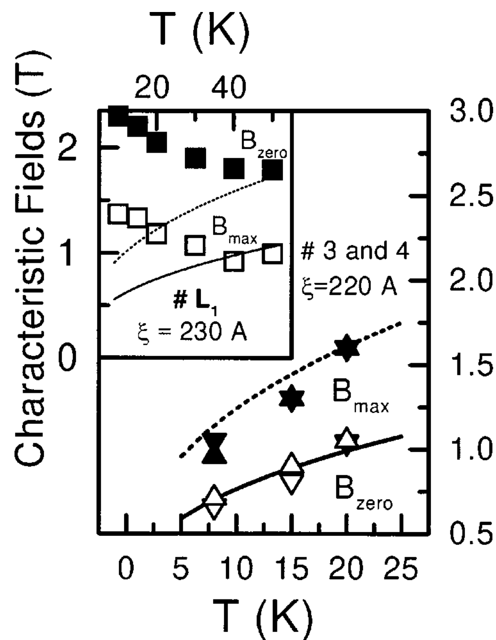


FIG. 11. Characteristic fields $B_{zero}$ and $B_{max}$ for samples No. 3, No. 4, and No. $L_1$ (inset). The dashed and solid lines are comparisons to calculations using a coherence length of 220 and 230 Å, respectively.

ized electrons (the localization length, the dielectric permeability, the width of the Coulomb gap, and the values of DOS at the Fermi level) are obtained by the analysis of the VRH conduction in zero field, on one hand, and PMR in a small field, on the other. The investigated samples can be divided into two groups (i) No. $L_1$ (and No. $L_2$) and (ii) No. 3 and No. 4. For the second group the results obtained with both methods are consistent, taking into account the conditions of their applicability. On the other hand, for No. $L_1$ the first (zero field) is found to be inapplicable, while the results found by the second one (PMR$\sim B^2$) agree reasonably well with those for the second group.

NMR in low fields is observed in all the specimens in both VRH regimes. It is interpreted as a result of quantum interference between different paths of the tunneling electron in conditions of scattering by intermediate centers. From the temperature dependence of the prefactor $f(T)$ of the low-field (quadratic) asymptote of NMR and those of the characteristic fields $B_{max}(T)$ and $B_{zero}(T)$ it has been established that again, the investigated samples can be divided into the same two groups depending on what kind of scattering (single or multiple scattering) takes place in the formation of NMR. The possible reason for this nonuniversal behavior lies in the different methods of the sample preparation. Residual implantation damage in $n$-$CuGaSe_2$ seems to dominate the properties of the localized electrons at low temperatures.

## ACKNOWLEDGMENTS

The authors would like to thank N. Fabre for Ge-ion implantation and M. Klenk, O. Schenker, J. Oestreich, U. Probst, Ch. Kloc, H. Riazi-Nejad, and V. Alberts for helpful discussions as well as technical assistance. Moreover, one of the authors (J.H.S.) is especially grateful to B. Batlogg for use of his equipment and continued support.

[1] M. Saad, E. Bucher, and M. Ch. Lux-Steiner, Appl. Phys. A: Mater. Sci. Process. **62**, 181 (1996).
[2] V. Nadenau, D. Hariskos, and H. W. Schock, *Proceedings of the 14th European Photovoltaic Solar Energy Conference, Barcelona* (Stephens, Bedford, UK, 1997), p. 1250.
[3] J. H. Schön, J. Oestreich, O. Schenker, H. Riazi-Najad, M. Klenk, N. Fabre, E. Arushanov, and E. Bucher, Appl. Phys. Lett. **75**, 2969 (1999).
[4] J. H. Schön, E. Arushanov, N. Fabre, and E. Bucher, Sol. Energy Mater. **61**, 417 (2000).
[5] E. Arushanov, J. H. Schön, H. Matsushita, and T. Takizawa, Phys. Status Solidi A **176**, 1009 (1999).
[6] N. F. Mott, *Metal-Insulator Transitions* (Taylor & Francis, London, 1974).
[7] N. F. Mott and E. A. Davies, *Electron Processes in Non-Crystalline Materials* (Clarendon, Oxford, 1979).
[8] B. I. Shklovskii and A. L. Efros, *Electronic Properties of Doped Semiconductors* (Springer, Berlin, 1984).
[9] A. N. Ionov, I. S. Shlimak, and M. N. Matveev, Solid State Commun. **47**, 763 (1983).
[10] K. G. Lisunov, E. K. Arushanov, Ch. Kloc, U. Malang, and E. Bucher, Phys. Status Solidi B **195**, 227 (1997).
[11] J. H. Schön, Ch. Kloc, E. Arushanov, G. A. Thomas, and E. Bucher, J. Phys.: Condens. Matter **12**, 4603 (2000).
[12] B. I. Shklovskii and B. Z. Spivak, in *Hopping Transport in Solids*, edited by M. Pollak and B. I. Shklovskii (North-Holland, Amsterdam, 1991), p. 271.
[13] E. Arushanov, K. G. Lisunov, U. Malang, Ch. Kloc, and E. Bucher, Phys. Rev. B **56**, 1005 (1997).
[14] W. Schirmacher, Phys. Rev. B **41**, 2461 (1990).
[15] M. E. Raikh and G. F. Wessels, Phys. Rev. B **47**, 15609 (1993).
[16] U. Sivan, O. Entin-Wohlmann, and Y. Imry, Phys. Rev. Lett. **60**, 1566 (1988).
[17] O. Entin-Wohlmann, Y. Imry, and U. Sivan, Phys. Rev. B **40**, 8342 (1989).
[18] L. Nguyen, B. Z. Spivak, and B. I. Shklovskii, Zh. Eksp. Teor. Fiz. **89**, 1770 (1985) [Sov. Phys. JETP **62**, 1021 (1985)].
[19] L. Essaleh, J. Galibert, S. M. Wasim, E. Hernandez, and J. Leotin, Phys. Rev. B **50**, 18040 (1994).
[20] E. Tremblay, M. Pepper, D. Ritchie, D. C. Peacock, J. E. Frost, and G. A. Jones, Phys. Rev. B **39**, 8059 (1989).
[21] Y. Zhang and M. P. Sarachik, Phys. Rev. B **43**, 7212 (1991).

**Downloaded 13 Apr 2004 to 130.232.104.240. Redistribution subject to AIP license or copyright, see http://jap.aip.org/jap/copyright.jsp**